



# Cytochrome P450 3A Enzymes Are Key Contributors for Hepatic Metabolism of Bufotalin, a Natural Constituent in Chinese Medicine Chansu

Zi-Ru Dai<sup>1†</sup>, Jing Ning<sup>2†</sup>, Gui-Bo Sun<sup>1</sup>, Ping Wang<sup>3</sup>, Feng Zhang<sup>3</sup>, Hong-Ying Ma<sup>3</sup>, Li-Wei Zou<sup>3</sup>, Jie Hou<sup>2</sup>, Jing-Jing Wu<sup>4</sup>, Guang-Bo Ge<sup>3,4\*</sup>, Xiao-Bo Sun<sup>1\*</sup> and Ling Yang<sup>3</sup>

<sup>1</sup> Key Laboratory of Bioactive Substances and Resources Utilization of Chinese Herbal Medicine, Ministry of Education, Institute of Medicinal Plant Development, Chinese Academy of Medical Sciences and Peking Union Medical College, Beijing, China, <sup>2</sup> College of Pharmacy, Dalian Medical University, Dalian, China, <sup>3</sup> Institute of Interdisciplinary Integrative Medicine Research, Shanghai University of Traditional Chinese Medicine, Shanghai, China, <sup>4</sup> Dalian Institute of Chemical Physics, Chinese Academy of Sciences, Dalian, China

## OPEN ACCESS

### Edited by:

Haitao Lu,  
Shanghai Jiao Tong University, China

### Reviewed by:

Caisheng Wu,  
Xiamen University, China  
Ying Xie,  
Macau University of Science  
and Technology, Macau

### \*Correspondence:

Guang-Bo Ge  
geguangbo@dicp.ac.cn  
Xiao-Bo Sun  
sun\_xiaobo@163.com

†These authors have contributed  
equally to this work

### Specialty section:

This article was submitted to  
Ethnopharmacology,  
a section of the journal  
Frontiers in Pharmacology

Received: 29 June 2018

Accepted: 18 January 2019

Published: 04 February 2019

### Citation:

Dai Z-R, Ning J, Sun G-B,  
Wang P, Zhang F, Ma H-Y, Zou L-W,  
Hou J, Wu J-J, Ge G-B, Sun X-B and  
Yang L (2019) Cytochrome P450 3A  
Enzymes Are Key Contributors  
for Hepatic Metabolism of Bufotalin,  
a Natural Constituent in Chinese  
Medicine Chansu.  
Front. Pharmacol. 10:52.  
doi: 10.3389/fphar.2019.00052

Bufotalin (BFT), one of the naturally occurring bufadienolides, has multiple pharmacological and toxicological effects including antitumor activity and cardiotoxicity. This study aimed to character the metabolic pathway(s) of BFT and to identify the key drug metabolizing enzyme(s) responsible for hepatic metabolism of BFT in human, as well as to explore the related molecular mechanism of enzymatic selectivity. The major metabolite of BFT in human liver microsomes (HLMs) was fully identified as 5 $\beta$ -hydroxybufotalin by LC-MS/MS and NMR techniques. Reaction phenotyping and chemical inhibition assays showed that CYP3A4 and CYP3A5 were key enzymes responsible for BFT 5 $\beta$ -hydroxylation. Kinetic analyses demonstrated that BFT 5 $\beta$ -hydroxylation in both HLMs and human CYP3A4 followed the biphasic kinetics, while BFT 5 $\beta$ -hydroxylation in CYP3A5 followed substrate inhibition kinetics. Furthermore, molecular docking simulations showed that BFT could bind on two different ligand-binding sites on both CYP3A4 and CYP3A5, which partially explained the different kinetic behaviors of BFT in CYP3A4 and CYP3A5. These findings are very helpful for elucidating the phase I metabolism of BFT in human and for deeper understanding the key interactions between CYP3A enzymes and bufadienolides, as well as for the development of bufadienolide-type drugs with improved pharmacokinetic and safety profiles.

**Keywords:** bufotalin, cytochrome P450 3A (CYP3A), hydroxylation, human liver microsomes (HLMs), docking simulations

**Abbreviations:** 5-HBFT, 5 $\beta$ -hydroxybufotalin; ABT, 1-aminobenzotriazole; APM, advanced protein modeling; BF, bufalin; BFT, bufotalin; CB, cinobufagin;  $CL_{int}$ , intrinsic clearance; CYP, cytochrome P450; ESI, electrospray ionization; HLM, human liver microsomes;  $K_m$ , apparent affinity; NADPH, nicotinamide-adenine dinucleotide phosphate; NMR, nuclear magnetic resonance; RB, resibufogenin; TCM, traditional Chinese medicine; UFLC-DAD, ultra-fast liquid chromatography-diode array detector;  $V_{max}$ , apparent maximum reaction velocity.

## INTRODUCTION

Chansu, also known as toad poison or toad venom (Krenn and Kopp, 1998), has been used as an effective constituent of some well-known Chinese medicine formulas and widely used for the treatment of various diseases, including infection, pain, swelling, heart failure, as well as many types of cancer (Ye et al., 2006; Gao et al., 2010). BFT, one of the bufadienolides isolated from ChanSu, has been intensively studied due to its diverse bioactivities, such as cardiotoxic, local anesthetic, blood pressure-stimulating, respiration and anticancer activities (Kamano et al., 1998; Yeh et al., 2003; Ma et al., 2009). Notably, more attention has been paid to BFT due to its dramatic anti-tumor activity, as previous structure-antitumor activity studies have showed an acetyl at C-16 position and a hydroxyl at the C-14 position could significantly enhance the anti-tumor activity of bufadienolides (Zhu et al., 2014). BFT induces apoptosis against hepatocellular carcinoma cells, where it is the most potent one among known bufadienolides, such as BF, telocinobufagin and CB (Zhang et al., 2012; Ning et al., 2015a). However, BFT and its analogs in Chansu are extremely cardiotoxic and could produce digitalis toxicity-like cardiac effects (Gowda et al., 2003). Additionally, as potent  $\text{Na}^+/\text{K}^+$ -ATPase inhibitors, these digoxin-like components have been shown to be involved in severe morbidity and high mortality (Mijatovic and Kiss, 2013). Therefore, investigations on the metabolic/clearance pathway(s) of BFT in humans are essential for clinical risk assessment of this toxic compound and BFT-containing TCMs.

Structurally, bufadienolides such as BF, BFT, CB, and RB possess a novel steroidal A/B *cis*, B/C *trans* and C/D *cis* ring juncture with a characteristic  $\alpha$ -pyrone ring at C-17 position and  $\beta$ -hydroxyl at the C-3 position (Feng et al., 2017). Notably, BFT is an ester derivative of BF with an additional acetyl group at the C-16 position. Our previous study demonstrated that CYP3A4, the most abundant P450 isoform expressed in human liver, played a predominant role in  $1\beta$ - or  $5\alpha$ -hydroxylations of BF, CB, and RB (Ma et al., 2011; Ge et al., 2013; Ning et al., 2015b). The isoform selectivity of CYP3A4 toward hydroxylations of these bufadienolides is very high, which is superior to the selectivity of CYP3A4 toward known steroid-type substrates, such as progesterone and testosterone (Zhang et al., 2008b). Unfortunately, the metabolic pathways of BFT in human tissues, as well as the effects of substituting groups at the bufadienolide scaffold on the selectivity and metabolic rates of P450 enzymes have not been well investigated.

In the present study, the phase I metabolic pathway(s) of BFT and its metabolic behaviors in human tissues was investigated for the first time. The major metabolite(s) of BFT and the key drug metabolizing enzyme(s) responsible for hepatic metabolism of BFT in human were fully characterized by a panel of standard techniques. The results demonstrated that CYP3A mediated  $5\beta$ -hydroxylation is the major metabolic pathway of BFT in human liver, but the enzymatic kinetic behaviors of BFT  $5\beta$ -hydroxylation in CYP3A4 and in CYP3A5 are much varied. To identify the contribution of each CYP isoform in BFT  $5\beta$ -hydroxylation, as well as to explore the effects of the C-16 acyl group at the bufadienolide scaffold on the selectivity

and metabolic rates of CYP3A enzymes, both experimental and computational techniques are used to explain the differential kinetic behaviors of BFT in CYP3A4 and CYP3A5. These findings are very helpful for elucidating the phase I metabolism of BFT in human, as well as for exploring the key interactions between CYP3A enzymes and bufadienolides.

## MATERIALS AND METHODS

### Ethics Statement

This study was carried out in accordance with the Declaration of Helsinki. The study protocol was approved by the Ethics Committee of Peking Union Medical College (Beijing, China).

### Chemicals and Reagents

BFT and BF were purchased from Shanghai Winherb Medical Technology Company (Shanghai, China). ABT, furafylline, sulfaphenazole, clomethiazole, omeprazole, 8-methoxypsoralen, ticlopidine, CYP3cide, glucose-6-phosphate dehydrogenase, D-glucose-6-phosphate, and  $\text{NADP}^+$  were obtained from Sigma (St. Louis, MO, United States). Montelukast, quinidine, ketoconazole was purchased from Jianglai Biotechnology Co., Ltd. (Shanghai, China). The pooled HLMs (from 50 donors, lot no. X008067) were obtained from Bioreclamation/IVT (Baltimore, MD, United States). A panel of baculovirus expressed human P450s (CYP1A1, 1A2, 2A6, 2A13, 2B6, 2C8, 2C9, 2C19, 2D6, 2E1, 3A4, 3A5, 4F2, and 4F3), co-expressing NADPH-CYP reductase and cytochrome b5 were obtained from BD Gentest Corp (Woburn, MA, United States). All chemicals and solvents were of analytical grade.

### Incubation Conditions

Human liver microsomes or CYPs were incubated with NADPH-generating system, which included  $\text{NADP}^+$  (1 mM), glucose-6-phosphate (10 mM), glucose-6-phosphate dehydrogenase (1 unit/ml), and 4 mM  $\text{MgCl}_2$  in 100 mM potassium phosphate buffer (pH 7.4) in a total incubation volume of 200  $\mu\text{l}$ . After a 3 min preincubation at  $37^\circ\text{C}$ , the reaction was initiated by the addition of NADPH-generating system and further incubated at  $37^\circ\text{C}$  for 30 min. The reaction was quenched with 100  $\mu\text{l}$  of ice-cold acetonitrile. The samples were chilled, spun at  $20,000 \times g$  for 20 min at  $4^\circ\text{C}$ . Aliquots of supernatants were then stored at  $-20^\circ\text{C}$  until analysis. All incubations throughout the study were done in three experiments conducted in duplicate with S.D. values generally below 10%.

### Analytical Instruments and Conditions

The samples were analyzed by means of the UFLC system, which equipped with an SIL-20ACHT auto sampler, a CBM-20A communications bus module, a DGU-20A3 in-line degasser, a CTO-20AC column oven, two LC-20AD pumps and an SPD-M20A photodiode array detector. BFT and its metabolites were separated by using a Shim-pack XR-ODS (75 mm  $\times$  2.0 mm, 2.2  $\mu\text{m}$ , Shimadzu) analytical column with an ODS guard column (5 mm  $\times$  2.0 mm, 2.2  $\mu\text{m}$ , Shimadzu). The mobile phase was comprised of  $\text{CH}_3\text{CN}$  (A) and 0.2% formic acid (B), and the

gradient profile was as follow: 0–2 min, 90–58% B; 2–8 min, 58–38% B; 8–10 min, 5% B; 10–13 min, balanced to 90% B. BFT and its metabolites (5-HBFT) were detected at 300 nm and quantified in accordance with the standard calibration curves.

Bufotalin and its metabolites were identified by using a Shimadzu LC-MS-2010EV (Kyoto, Japan) instrument with an ESI interface. With regard to mass detection, positive-ion mode (ESI+) as well as negative ion mode (ESI-) from *m/z* 100–800 with the electron voltage setting at +1.55 kV, and –1.55 kV was employed. Data processing was conducted using the LC-MS Solution (version 3.41; Shimadzu).

## Biosynthesis and Characterization of BFT Metabolite

The major metabolite of BFT was biosynthesized using liver microsomes from mouse (MLM, 90%) and human (HLM, 10%) with respect to the incubation system up to 250 mL. BFT (200  $\mu$ M) was incubated with the liver microsomes (1.0 mg/mL) supplemented with the NADPH-generating system for 4 h at 37°C. Under these conditions, approximately 40% of BFT was converted into 5-HBFT. Then, BFT and its metabolite were separated by the HPLC (SHIMADZU, Kyoto, Japan) with a C18 column (4.6 mm  $\times$  150 mm, 10  $\mu$ m). The mobile phase was 65% methanol in water. The eluent was monitored at 300 nm with a flow rate of 1.5 mL/min, and the fractions containing 5-HBFT were collected and eluted in vacuo. The purity of metabolite was above 98% according to HPLC-UV analysis. NMR spectra were carried on a Varian INOVA-400 NMR spectrometer (Varian, United States). The purified metabolite was dissolved in CDCl<sub>3</sub> (Euriso-Top, Saint-Aubin, France), and chemical shifts were reported on  $\delta$  scale with reference to tetramethylsilane (TMS) at 0 ppm for <sup>1</sup>H-NMR (400 MHz) and <sup>13</sup>C-NMR (100 MHz).

## Reaction Phenotyping Assays With Recombinant CYPs

Fifteen cDNA-expressed human P450 isoforms co-expressing NADPH-P450 reductase were used for assay of BFT hydroxylation activity. Each of the recombinant CYPs (40–80 nM) were incubated with 3 and 100  $\mu$ M substrate concentrations (approximate concentration at  $V_{max}$ , and  $K_m$  values for HLM, respectively) at 37°C for 30 min.

## Chemical Inhibition Assays

5 $\beta$ -hydroxylation of BFT in pooled HLM was carried out by adding selective inhibitors. In brief, BFT (10  $\mu$ M, relevant to the  $K_m$  values) was incubated with or without known CYP isoform-specific inhibitors using a protein concentration of 0.25 mg protein/ml in HLM with an NADPH-generating system. The selective inhibitors and their concentrations were referred to the previous studies (Balani et al., 2002; Bjornsson et al., 2003; Feng et al., 2014).

## Kinetics Analyses

The formation rates of 5-HBFT was within the linear range of the incubation time and protein concentration. The required concentrations of BFT ranged from 10 to 250  $\mu$ M. BFT was

incubated with pooled HLM (0.25 mg protein/mL) for 30 min, or with recombinant CYP3A4 (5 nM) and CYP3A5 (10 nM) for 30 min. The apparent  $K_m$  and  $V_{max}$  values were determined by fitting experimental data to the Biphasic Kinetics equation (Eq. 1) and Substrate Inhibition equation (Eq. 2). The kinetic constants were calculated with GraphPad Prism software, version 6.0, and the results were graphically represented by Eadie–Hofstee plots.

$$v = \frac{V_{max1} [S]}{K_{max1} + [S]} + \frac{V_{max2} [S]}{K_{max2} + [S]} \quad (1)$$

where  $v$  is the rate of the reaction,  $[S]$  is the substrate concentration,  $V_{max}$  is the maximum velocity estimate,  $K_m$  is the substrate affinity constant.

$$v = \frac{V_{max}}{1 + (K_m/[S]) + ([S]/K_{si})} \quad (2)$$

where  $K_{si}$  is the substrate inhibition constant.

## Correlation Studies

The formation rates of the metabolite(s) described for BFT (50  $\mu$ M) were measured in a panel of 12 HLMs from individuals after 15–60 min incubation in HLM (0.25 mg protein/ml). These values were correlated with the levels of CYP3A4 or CYP3A5 as well as the catalytic activities of CYP3A4 to their marker substrates. BF was an isoform-specific probe substrate, which was first reported by our laboratory and its structure was similar with BFT. BF and its hydroxylation product were determined by LC-UV at 300 nm. The concentrations of CYP3A4 and CYP3A5 in HLMs were determined using MRM mode and SIL as the reference standards. Specific peptides of EVTNFLR (for CYP3A4) and SLGPVGFMK (for CYP3A5) were selected for their quantification by using transition ion of 439.7/549.3 and *m/z* 468.3/678.5, respectively (Liu et al., 2014). The correlation coefficient was expressed by the linear regression coefficient ( $R^2$ ).  $P < 0.005$  was considered statistically significant.

## Molecular Docking Simulations

Docking simulations were performed by using SYBYL (X-1.1) (Tripos, St. Louis, MO, United States) to generate active conformations by exploring all calculations of binding interactions and conformations of ligands. Here, the X-ray crystallographic structure of CYP3A4 (PDB ID:3TJS) and CYP3A5 (PDB ID:5VEU) were selected for docking analysis (Sevrioukova and Poulos, 2012; Hsu et al., 2018). A low-energy conformation with no steric clashes between side chains was energy minimized for 10,000 steps with the backbone and variable modeling. Surflex-Dock used an empirical scoring function and a patented search engine to generate the bioactive binding poses of substrates in the active site of CYP3A4 and CYP3A5. During the docking simulation, the enzyme structure was kept rigid, while the substrate was left fully flexible by changing the conformations of the ligand in the active site. With the crystal structure of 3A4 and 3A5, a total of 50 bioactive binding conformations of BFT were generated by means of Surflex-Dock, which were evaluated by an empirical function of ChemScore (Ai et al., 2010). The best bioactive poses selected

from the top ten solutions were then used for the analysis of the binding interactions between CYP3A and their substrates.

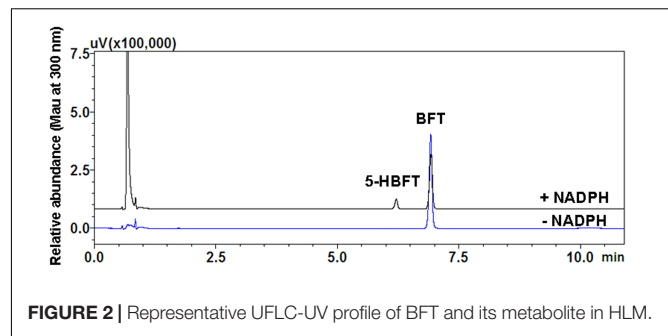
## RESULTS

### Biotransformation of BFT by Human Liver Microsomes

A single metabolite of BFT was identified following incubation with HLM (0.3 mg protein/ml) in the presence of the NADPH-generating system (Figure 1). As shown in Figure 2, one major product peak was eluted at 6.2 min. The metabolite was characterized by UFLC-DAD-ESI-MS, and the formation of monohydroxybufotalin was NADPH-, time-, and microsome-dependent. The material balance data has also demonstrated the uniqueness of this metabolite (Supplementary Figure S2 and Supplementary Table S1). The  $[M+H]^+$  and  $[M+CH_3CN+H]^+$  ion of the metabolite at  $m/z$  in HLM were 461.3 and 502.4, respectively. The molecular weight (MW) of metabolite was correspondingly calculated as 460, suggesting that this metabolite was a monohydroxylated product of BFT.

### Identification of the Major Metabolite of BFT

For elucidating the metabolic labile sites of BFT, this monohydroxylated metabolite was biosynthesized and further characterized based on  $^1H$ -NMR and  $^{13}C$ -NMR analysis (Table 1). In comparison with  $^{13}C$ -NMR spectrum of BFT to that of this metabolite, the additional oxygenated quaternary carbon at  $\delta$  73.53 (CH) was observed instead of tertiary carbon at  $\delta$  35.59 (C-5). For the meantime, three carbon signals (C-4, C-6, and C-10) presented corresponding shifts ( $\delta$  33.30– $\delta$  36.98,  $\delta$  26.40– $\delta$  35.14, and  $\delta$  35.60– $\delta$  40.76, respectively). The upfield shifts of C-1 ( $\delta$  64.04) and C-19 ( $\delta$  76.08) were observed owing to the *g*-gauche effect, indicating that hydroxylation occurred at the C-5 site. Moreover, the NMR data of metabolite were consistent with the previously reported spectral data of marinobufagenin (Zhang et al., 2011). Based on above findings, the hydroxylated metabolite was fully identified as 5 $\beta$ -hydroxybufotalin.



### Reaction Phenotyping Assays

In order to explore the involved P450 isoform(s) for the metabolism of BFT in humans, the formation of 5-HBFT was evaluated using a series of P450 isoforms. As shown in Figure 3, one hydroxylated metabolite was mediated specifically by CYP3A4 and CYP3A5, while no metabolites were detected in the incubation systems with other P450 isoforms. The formation rates of 5-HBFT in CYP3A4 were  $1.30 \pm 0.05$  and  $10.50 \pm 0.42$  per min/nmol P450 upon addition of BFT with the substrate concentrations of 3 and 100  $\mu$ M, respectively. In contrast, the BFT 5 $\beta$ -hydroxylation rates in CYP3A5 were relatively slow, with the 5-HBFT formation rates were  $1.08 \pm 0.08$  and  $3.42 \pm 0.07$  per min/nmol P450, respectively.

### Chemical Inhibition Assays

To further verify the key P450 isoform(s) involved in the formation of 5-HBFT in HLM, chemical inhibition assays were conducted by using a panel of selective inhibitors of major P450 isoforms. As shown in Figure 4, ABT (a broad P450 inhibitor) could inhibit the formation of 5-HBFT completely, indicating that BFT hydroxylation was highly P450-specific. Among all tested isoform-selective inhibitors, ketoconazole (CYP3A inactivator) completely inhibited the catalytic activity of HLM, further indicating CYP3A played the conspicuous role in BFT hydroxylation. Moreover, CYP3cide, an exclusive inhibitor of CYP3A4, could inhibit  $\sim$ 90% formation of 5 $\beta$ -hydroxybufotalin in HLM, suggesting that CYP3A4 is the

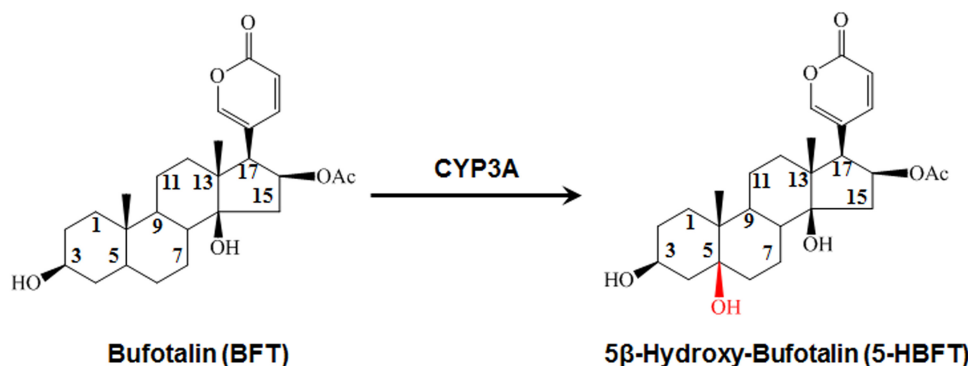


FIGURE 1 | The 5 $\beta$ -hydroxylation of BFT in HLM.

**TABLE 1** | Proton and carbon NMR chemical shift assignments for BFT and its metabolite.

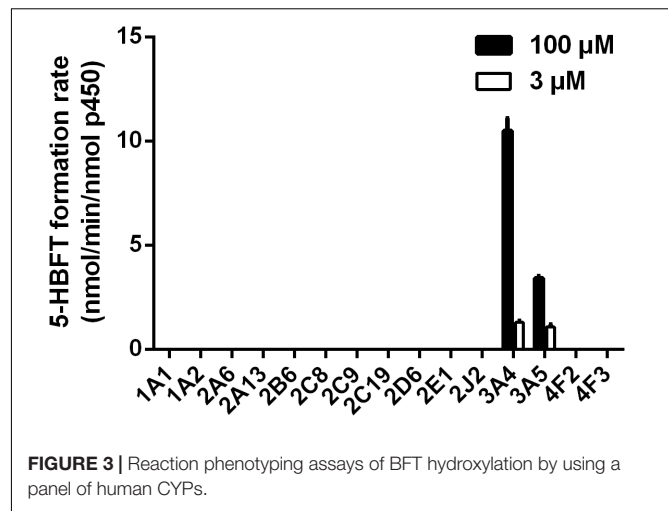
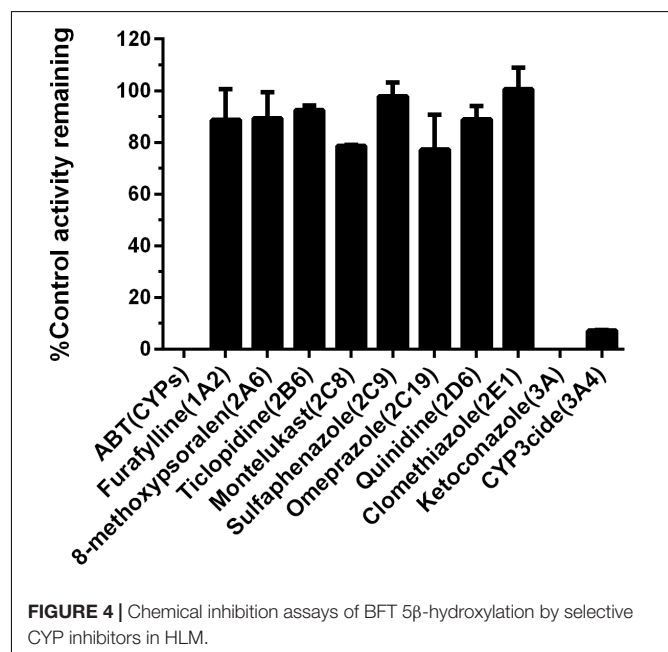
Position	5 $\beta$ -Hydroxy-Bufotalin		Bufotalin	
	$\delta$ 1H Mult (J in Hz)	$\delta$ 13C	$\delta$ 1H Mult (J in Hz)	$\Delta$ 13C
1	1.16	23.6	1.19	29.6
	1.94		1.91	
2	1.38	24.8	1.28	27.9
	1.83		1.59	
3	4.20	68.1	4.14	66.7
4	1.56	36.9	1.24	33.3
	2.11		1.76	
5	–	73.5	1.59	35.9
6	1.47	35.1	1.46	26.4
	1.72		1.79	
7	1.28	21.5	1.32	21.1
	1.47		1.43	
8	1.50	39.1	1.49	42.3
9	1.57	41.4	1.56	35.3
10	1.83	40.7	1.84	35.6
11	1.61	28.7	1.54	21.1
	–		1.36	
12	1.25	40.5	1.39	40.9
	1.59		1.50	
13	–	49.3	–	49.4
14	–	84.4	–	84.4
15	2.85	57.1	1.53	40.4
			2.65	
16	5.52	74.4	5.54	73.6
17	2.59	40.8	2.87	57.2
18	0.79	16.4	0.79	16.4
19	0.95	16.7	0.95	23.7
20	–	116.7	–	116.9
21	7.25	151.1	7.25	151.0
22	8.00	149.0	8.03	149.2
23	6.19	113.2	6.19	113.1
24	–	161.9	–	161.9
25	–	170.0	–	170.0
26	1.87	20.9	1.87	20.9

All spectra were recorded on a Bruker ARX-600 spectrometer, in CDCl<sub>3</sub>.

predominant enzyme accountable for BFT 5 $\beta$ -hydroxylation. In contrast, the selective inhibitors against other P450 isoforms did not show significant inhibitory effects (less than 25% inhibition,  $P > 0.05$ ) on this biotransformation. These results suggested that BFT was selectively metabolized by CYP3A, while CYP3A4 play a key role in the formation of 5 $\beta$ -hydroxybufotalin in human liver.

## Kinetic Analyses

Over the entire concentration range examined, the kinetics behaviors of 5 $\beta$ -hydroxylation of BFT, in HLM and CYP3A4 followed the biphasic kinetics, but this reaction obeyed the

**FIGURE 3** | Reaction phenotyping assays of BFT hydroxylation by using a panel of human CYPs.**FIGURE 4** | Chemical inhibition assays of BFT 5 $\beta$ -hydroxylation by selective CYP inhibitors in HLM.

substrate inhibition kinetic in CYP3A5, as evidenced by Eadie-Hofstee plot (**Figure 5**). In addition, the similar apparent kinetic parameters were observed in the kinetic characterization of BFT 5 $\beta$ -hydroxylation in HLM and CYP3A4. In HLM,  $K_{m1}$  and  $K_{m2}$  values for the formation of 5-HBFT were 3.71 and 133.70  $\mu$ M, respectively, while the  $V_{max1}$  and  $V_{max2}$  values for 5-HBFT formation were 33.31 and 107.30 per min/mg, respectively. Similarly, the  $K_{m1}$  and  $K_{m2}$  values of BFT 5 $\beta$ -hydroxylation by CYP3A4 were 3.46 and 122.40  $\mu$ M, respectively, whereas the values of  $V_{max1}$  and  $V_{max2}$  were 6.87 and 33.70 per min/nmol P450, respectively (**Table 2**). In CYP3A5, the  $K_m$  and the  $K_i$  value for the formation of 5-HBFT was 2.91 and 170.00  $\mu$ M, the corresponding  $V_{max}$  value was 3.45 nmol/min per nanomole P450. These results implied that BFT displayed different kinetic behaviors in CYP3A4 and CYP3A5.

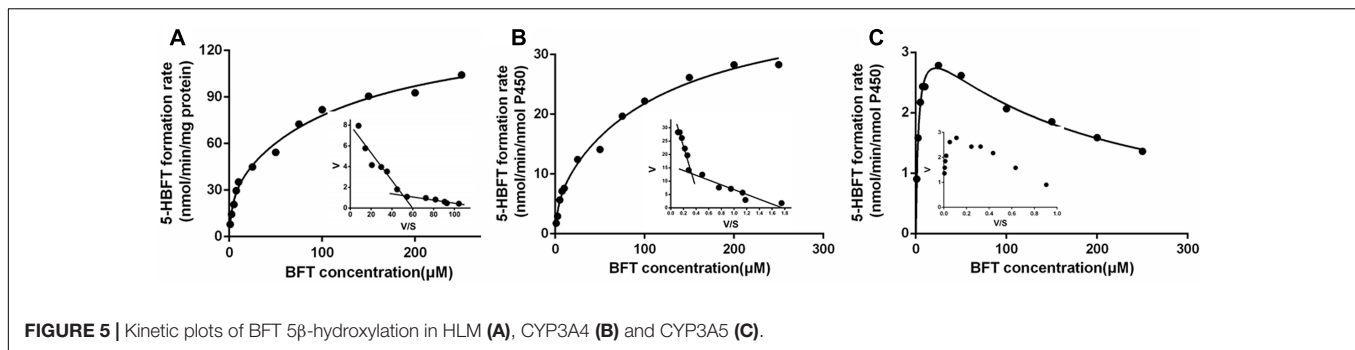


**FIGURE 5** | Kinetic plots of BFT 5 $\beta$ -hydroxylation in HLM (A), CYP3A4 (B) and CYP3A5 (C).

## Correlation Studies

It is well-known that CYP3A4 and CYP3A5 are two major CYP3A isoforms distributed in adult human liver, and these two enzymes share high amino acid sequence identity (>84%). Generally, the abundance of CYP3A5 is relative lower than that of CYP3A4 in human liver. Thus, in most cases, CYP3A4 has been considered to be a key determinant crucial for the hepatic metabolism of CYP3A substrates. In this study, the correlations between the expression levels of CYP3A4 or CYP3A5 expression levels and BFT hydroxylation were carefully studied to reveal which isoenzyme was the major enzyme responsible for hepatic metabolism of BFT (Daly, 2006). To this end, the determination of the formation rates of 5-HBFT were using a panel of 12 HLMs from different individual donors, while the proteins levels of CYP3A4 or CYP3A5 were also determined by a proteomics-based method. After that, the formation rates of 5-HBFT were compared with the protein levels of CYP3A4 or CYP3A5 in individual HLMs. As shown in **Figures 6A,B**, a strong linear regression coefficient ( $R^2$ ) between the formation rates of 5-HBFT and the expression levels of CYP3A4 in individual HLMs ( $R^2 = 0.8966$ ,  $P < 0.001$ ) was observed, while the formation rates of 5-HBFT is poorly correlated with the CYP3A5 levels ( $R^2 = 0.2256$ ,  $P = 0.1187$ ). Furthermore, the CYP3A activities in individual HLMs measured by using BFT was also compared with the CYP3A4 activities determined by BE, a previously reported isoform-specific probe substrate for CYP3A4. As shown in **Figure 6C**, a splendid correlation between

the formation rates of 5-HBFT and the formation rates of 5-HBF was observed ( $R^2 = 0.8799$ ,  $P < 0.001$ ). These findings suggested that CYP3A4 played a key role in BFT 5 $\beta$ -hydroxylation in HLM from Mongolian Populations.

## Molecular Docking Simulations

For further providing deep insights into CYP3A-mediated BFT 5 $\beta$ -hydroxylation, molecular modeling simulations were performed from the perspective of recognition and binding between the substrate and two CYP3A enzymes. It is well-known that the active cavity of both CYP3A4 and CYP3A5 are relatively large and flexible, both enzymes have been identified with more than two different ligand-binding sites (Isin and Guengerich, 2006). As shown in **Figure 7**, the active cavity of both CYP3A4 and CYP3A5 could accommodate two molecular substrates (BFT). In CYP3A4, two BFT molecules are stacked in a parallel orientation, the first one (BFT) could be well-docked into the catalytic site with the H atom of the C-5 site facing the heme iron at 4.35 Å, while the second one could bind on the surrounding area near to the first one with relatively far site-heme distance (11.00 Å). The closer BFT to the heme in the model will be termed active BFT, while the other BFT molecule will be termed effector BFT. The results indicated that the active BFT would facilitate the subsequent binding effector BFT. In contrast, the binding areas of two molecules of BFT in CYP3A5 were highly overlapped, the active BFT lied against the effector BFT molecule in the CYP3A4 active site with site-heme distance 5.49 and 7.18 Å. The presence of the effector BFT molecule shifted active BFT away from the heme, and the molecule no longer rotated freely in the active site, implying that the binding of the effector molecule would affect the binding of the active substrate in CYP3A5 (**Table 3**). In addition, the acetate group at the C-16 site of active BFT formed hydrogen bonds with the Glu374 of both CYP3A4 and CYP3A5, which could fix the active substrate in a favorable position for the further metabolic reaction, indicating that the acetate group may play a critical role in positioning the active substrates in recognition and binding of CYP3A enzymes. Moreover, Glu374 seemed to be important for CYP3A specificity (**Figures 7C,D**). These findings agreed well with the experimental data and could partly explain why BFT 5 $\beta$ -hydroxylation displayed the autoactivation kinetics in CYP3A4, while in CYP3A5, obeyed the substrate inhibition kinetics.

**TABLE 2** | Kinetic parameters of BFT 5 $\beta$ -hydroxylation in HLM, recombinant human CYP3A4 and CYP3A5.

Enzyme Source	High-affinity site		Low-affinity site	
	$V_{max}$	$K_m$	$V_{max}$	$K_m$
HLM	33.31 $\pm$ 12.64	3.71 $\pm$ 2.68	107.30 $\pm$ 11.77	133.70 $\pm$ 72.23
CYP3A4	6.87 $\pm$ 3.59	3.46 $\pm$ 3.51	33.70 $\pm$ 3.08	122.40 $\pm$ 56.5
	$V_{max}$	$K_m$	$K_{si}$	$CL_{int}$
CYP3A5	3.45 $\pm$ 0.09	2.91 $\pm$ 0.24	170.00 $\pm$ 12.69	1186.12

$K_m$  values are  $\mu M$ ,  $V_{max}$  values are  $nmol \cdot min^{-1} \cdot mg^{-1}$  for liver microsomes or  $nmol \cdot min^{-1} \cdot nmol^{-1}$  of P450 for CYP3A. The range of substrate concentrations was 1–250  $\mu M$ . Each value was the mean  $\pm$  S.D. of three determinations performed in duplicate.

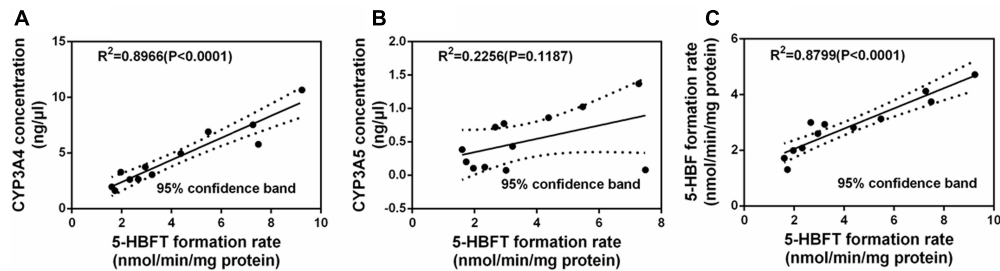


**FIGURE 6 |** Correlation studies between the formation rates of 5-HBFT and the levels of CYP3A4 (A), or the levels of CYP3A5 (B), and the formation rates of 5-HBFT (C), in a panel of twelve HLMs from individuals.

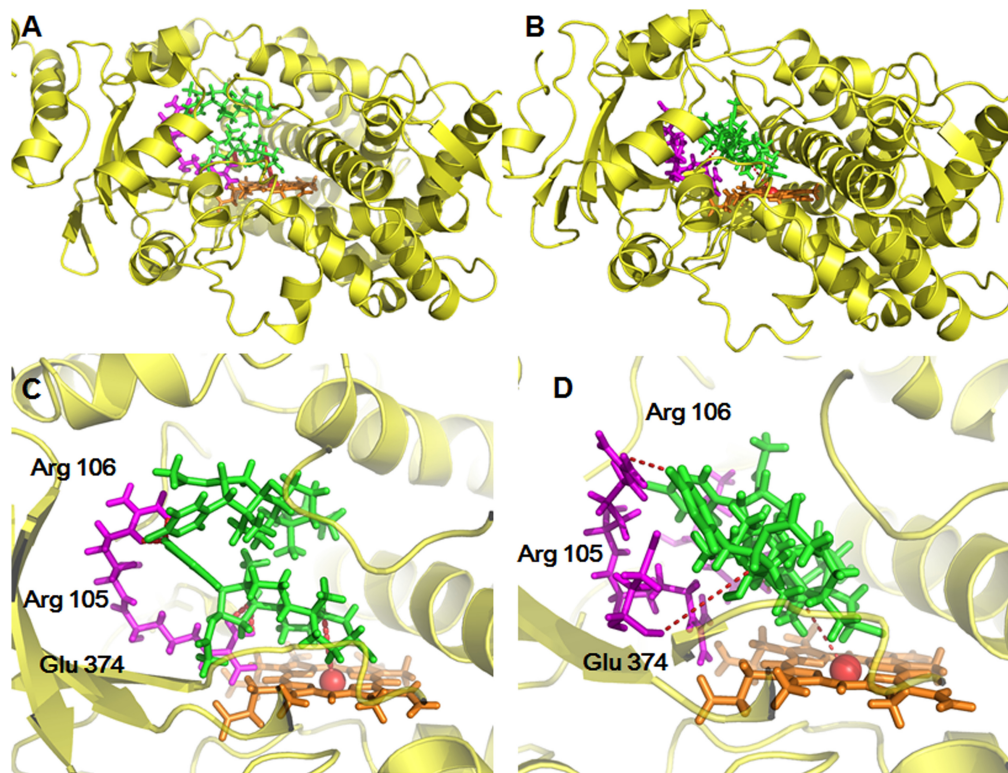


**FIGURE 7 |** The stereo views of docking simulations of BFT into the active cavity of both CYP3A4 (A) and CYP3A5 (B). The detailed views of the binding areas showed that BFT on CYP3A4 and CYP3A5, while BFT could docked into different ligand binding site of CYP3A4 (C) and CYP3A5 (D).

## DISCUSSION

As a biologically active compound of the bufadienolides isolated from ChanSu, BFT has drawn increasing attentions in recent

years especially for its anticancer effects. Recent studies have revealed that BFT could regulate a variety of cellular activities, such as proliferation, differentiation, apoptosis, as well as glucose metabolism, angiogenesis and multidrug resistance in human tumors (Dong et al., 2011; Salvador et al., 2013). Therefore, it is highly desirable to fully characterize the metabolic pathway(s) of BFT to expedite the process for the drugability assessment of this bufadienolide. Although the metabolic pathways of BFT in mice and in some microorganisms have been reported (Xin et al., 2009; Li et al., 2011; Huang et al., 2015), the metabolic pathways of BFT in human tissues have not been reported yet. In this study, the metabolite profile of BFT in HLMs has been well studied and the major metabolite and the involved metabolic enzymes have

**TABLE 3 |** BFT 5 $\beta$ -hydroxylation related parameters derived from the molecular modeling of BFT with the crystal complex of CYP3A4 and CYP3A5, respectively.

Parameters	CYP3A4 (near)	CYP3A4 (far)	CYP3A5 (near)	CYP3A5 (far)
Hammerhead score	-33.70	-18.96	-26.88	-22.14
Site-heme distance	4.35 Å	11.00 Å	5.49 Å	7.18 Å

been identified for the first time. Our results clearly demonstrated that BFT could be readily catalyzed by CYP3A4 and CYP3A5 to 5-HBFT in HLM, which is consistent with the metabolic pathway(s) of BFT in mice. However, the catalytic efficacy and the kinetic behaviors of BFT 5 $\beta$ -hydroxylation are quite different in CYP3A4 and CYP3A5. Taking into account that CYP3A enzymes are the predominant contributors in hepatic metabolism of BFT, the individual discrepancy in BFT metabolism may be very significant due to the large inter-individual differences in the expression and function of CYP3A (Liu et al., 2017). Although the levels of CYP3A4 in liver is generally higher than CYP3A5, but in some cases, the levels of CYP3A5 in given populations (such as African) may higher than that of CYP3A4 (Westlind-Johnsson et al., 2003; Lu et al., 2012). Given that the relative content of CYP3A5 to total hepatic CYP3A protein varies remarkably among individuals (17–50%), the contribution of CYP3A5 in BFT metabolism and the kinetic behaviors of BFT 5 $\beta$ -hydroxylation may be strongly affected by the expression and function of CYP3A5 (Wu et al., 2016).

Our previous studies have found that CYP3A4 played a leading role in hydroxylations of bufadienolides (**Supplementary Figures S1, S3**) (Ma et al., 2011; Ge et al., 2013). However, the present study demonstrated that the increased contribution of CYP3A5 was involved in BFT 5 $\beta$ -hydroxylation in comparison with other naturally occurring bufadienolides. Docking simulations demonstrated that the distance between the H atom of the C-5 site and the heme of CYP3A4 of BF was shorter than that in CYP3A5, while the bioactive pose of BF in 3A4 given higher hammerhead score values than that in 3A5. These findings agreed well with the experimental results, in which BF 5 $\beta$ -hydroxylation catalyzed by CYP3A4 was easier than that by CYP3A5 (**Supplementary Figure S4 and Supplementary Table S2**). The improved CYP3A5 preference could be attributed to their subtle structural differences at the C-16 site. From the views of the chemical structure, the acetyl substituent group has been introduced into the specific carbon of bufadienolides, which may affect the isoform selectivity and the kinetics behaviors of 5 $\beta$ -hydroxylation in both CYP3A4 and CYP3A5. It was apparent from **Figure 4** and **Table 2** that BFT 5 $\beta$ -hydroxylation in HLM and CYP3A4 followed the biphasic kinetics, while in CYP3A5, obeyed the substrate inhibition kinetics, which differed from BF formed mono-hydroxylated metabolites and followed Michaelis–Menten kinetics in CYP3A4 (**Supplementary Table S3**). These results suggest that the presence of acetyl substituent group at C-16 site may affect the binding and catalytic process between BFT and CYP3A4 and CYP3A5. It has been reported CYP3A subfamily, which has large substrate-binding pockets, is competent to bind two or more molecules of same substrates that exhibit homotropic or heterotropic cooperativity (Yusuke et al., 2008; Zhang et al., 2008a; Davydov et al., 2012; Raunio et al., 2015). Both kinetic analyses and docking simulations demonstrated that the introduction of the acetyl substituent group, a hydrophilic radical would contribute to BFT bind with two different ligand binding site of both CYP3A4 and CYP3A5, especially through the formation of H-bond with the residual Glu374, which then led to different allosteric effects (Cameron et al., 2005; Sohl et al., 2008).

The binding of active BFT molecule (the closer BFT to the heme) to CYP3A4 was deemed to make effector BFT restrain in a stacked parallel configuration, which triggered a structural transition that facilitated the succedent binding event(s), whereas an opposite structural transition that slowed down the progress of binding event(s) when BFT molecule bound to CYP3A5, the presence of the effector BFT molecule shifted active BFT away from the heme, in turn resulting in different catalytically competent enzyme-substrate complexes.

The different kinetic behaviors of BFT-hydroxylation in both CYP3A4 and CYP3A5 could also be attributed to the distinctions of the active site of CYP3A4 and CYP3A5. Although the secondary and tertiary structures of CYP3A5 have a strong resemblance of CYP3A4, the CYP3A5 active site is relatively taller and narrower than that of CYP3A4, which may affect the substrate-binding process (Emoto and Iwasaki, 2006; Hsu et al., 2018). Previous study indicated that the narrow cavity and position of Glu374 probably contribute to the higher selectivity of 3A5 over 3A4 for the O-demethylation of schisantherin E (Wu et al., 2017). In present study, the docking study also verified that the binding of the active BFT to the narrower active site of CYP3A5 triggered contractions through the hydrogen bonds with the Glu374, which made the binding areas of two molecules of BFT highly overlap. By contrast in CYP3A4, the active BFT could be well-docked into the catalytic site, which expanded the active site cavity that enabled the effector BFT to bind on the surrounding area near to the active molecule. Therefore, these findings might be able to explain why BFT 5 $\beta$ -hydroxylation displayed the autoactivation kinetics in CYP3A4, while in CYP3A5, obeyed the substrate inhibition kinetics.

The structure-activity relationship studies revealed bio-transformation of bufadienolides could remarkably alter the cytotoxic activities, especially hydroxylated products showed even more potent activity than their precursors against cancer cell (Ye et al., 2004). Our previous studies demonstrated that CYP3A-mediated RB 5 $\beta$ -hydroxylation in humans produces the bioactive metabolite marinobufagenin with superior metabolic stability, implying that RB might be useful as a prodrug whose anticancer effects *in vivo* could still be preserved after biotransformation (Ning et al., 2015b). Likewise, 5 $\beta$ -hydroxyl BFT may show similar or even more potent cytotoxicities comparable to BFT. Recent studies demonstrated that all metabolites achieved similar maximum tumor inhibition rates as BFT regardless of hydroxylation or dehydrogenation, which suggested BFT could be considered as a potential leading anticancer agent (Han et al., 2016). Therefore, BFT presents a promising antitumor potential and deserves further investigation.

## CONCLUSION

In summary, the phase I metabolic pathways of BFT has been carefully characterized. The major metabolite of BFT in HLM was purified and fully identified as 5 $\beta$ -hydroxylbufotalin, while CYP3A4 and CYP3A5 were the major isoform responsible for BFT 5 $\beta$ -hydroxylation. BFT 5 $\beta$ -hydroxylation in both HLM and CYP3A4 obeyed the biphasic kinetics, while such

biotransformation in CYP3A5 followed the substrate inhibition kinetics. Molecular docking simulations were also performed to explore the interactions between BFT and CYP3A, and the results demonstrated that BFT could bind on two different ligand-binding sites including one high-affinity and one low affinity site on both CYP3A4 and CYP3A5, which was very different from other natural occurring bufadienolides including BF and CB. All these findings suggested that CYP3A-mediated 5 $\beta$ -hydroxylation was the major metabolic pathway of BFT in the human liver, while the acyl substituent group at C-16 site of bufadienolides could affect the catalytic behaviors and enzyme specificity of bufadienolides.

## AUTHOR CONTRIBUTIONS

Z-RD and JN were involved in the project design, carried out most of the experiments, and drafted the manuscript. G-BS, J-JW, H-YM, and FZ contributed to the data analysis. PW, L-WZ, and JH participated in the biosynthesis and characterization of metabolite. G-BG, X-BS and LY designed and supervised this study. All authors read and approved the manuscript finally.

## REFERENCES

- Ai, C. Z., Li, Y., Wang, Y. H., Li, W., Dong, P. P., Ge, G. B., et al. (2010). Investigation of binding features: effects on the interaction between CYP2A6 and inhibitors. *J. Comput. Chem.* 31, 1822–1831. doi: 10.1002/jcc.21455
- Balani, S. K., Zhu, T., Yang, T. J., Liu, Z., He, B., and Lee, F. W. (2002). Effective dosing regimen of 1-aminobenzotriazole for inhibition of antipyrine clearance in rats, dogs, and monkeys. *Drug. Metab. Dispos.* 30, 1059–1062. doi: 10.1124/dmd.30.10.1059
- Bjornsson, T. D., Callaghan, J. T., Einolf, H. J., Fischer, V., Gan, L., Grimm, S., et al. (2003). Manufacturers of america drug metabolism/clinical pharmacology technical working, the conduct of in vitro and in vivo drug-drug interaction studies: a PhRMA perspective. *J. Clin. Pharmacol.* 43, 443–469. doi: 10.1177/0091270003252519
- Cameron, M. D., Wen, B., Allen, K. E., Roberts, A. G., Schuman, J. T., Campbell, A. P., et al. (2005). Cooperative binding of midazolam with testosterone and alpha-naphthoflavone within the CYP3A4 active site: a NMR T-1 paramagnetic relaxation study. *Biochemistry* 44, 14143–14151. doi: 10.1021/bi051689t
- Daly, A. K. (2006). Significance of the minor cytochrome P450 3A isoforms. *Clin. Pharmacokinet.* 45, 13–31. doi: 10.2165/00003088-200645010-00002
- Davydov, D. R., Rumpf, J. A. O., Sineva, E. V., Fernando, H., Davydova, N. Y., and Halpert, J. R. (2012). Peripheral ligand-binding site in Cytochrome P450 3A4 located with Fluorescence Resonance Energy Transfer (FRET). *J. Biol. Chem.* 287, 6797–6809. doi: 10.1074/jbc.M111.325654
- Dong, Y., Yin, S., Li, J., Jiang, C., Ye, M., and Hu, H. (2011). Bufadienolide compounds sensitize human breast cancer cells to TRAIL-induced apoptosis via inhibition of STAT3/Mcl-1 pathway. *Apoptosis* 16, 394–403. doi: 10.1007/s10495-011-0573-5
- Emoto, C., and Iwasaki, K. (2006). Enzymatic characteristics of CYP3A5 and CYP3A4: a comparison of in vitro kinetic and drug-drug interaction patterns. *Xenobiotica* 36, 219–233. doi: 10.1080/00498250500489968
- Feng, R., Zhou, X. L., Tan, X. S., Or Penelope, M. Y., Hu, T., Fu, J., et al. (2014). In vitro identification of cytochrome P450 isoforms responsible for the metabolism of 1-hydroxyl-2,3,5-trimethoxy-xanthone purified from *Halenia elliptica* D. Don. *Chem. Biol. Interact.* 210, 12–19. doi: 10.1016/j.cbi.2013.12.008
- Feng, Y. J., Wang, C., Tian, X. G., Huo, X. K., Feng, L., Sun, C. P., et al. (2017). In vitro phase I metabolism of gamabufotalin and arenobufagin: reveal the effect of substituent group on metabolic stability. *Fitoterapia*. 121, 38–45. doi: 10.1016/j.fitote.2017.06.022

## FUNDING

This work was supported by the National Key Research and Development Program of China (2017YFC1700200 and 2017YFC1702000), the NSF of China (81573501, 81773810, 81773687, 81503152, and 81803627), Program of Shanghai Academic/Technology Research Leader (18XD1403600), Shuguang Program (18SG40) supported by Shanghai Education Development Foundation and Shanghai Municipal Education Commission, Beijing Natural Science Foundation (7184229), CAMS Innovation Fund for Medical Sciences (CIFMS) (2017-I2M-1-013), PUMC Youth Fund and the Fundamental Research Funds for the Central Universities (2017350015), and China Postdoctoral Science Foundation funded project (2017M610063 and 2018T110072).

## SUPPLEMENTARY MATERIAL

The Supplementary Material for this article can be found online at: <https://www.frontiersin.org/articles/10.3389/fphar.2019.00052/full#supplementary-material>

- Gao, H., Popescu, R., Kopp, B., and Wang, Z. (2010). Bufadienolides and their antitumor activity. *Nat. Prod. Rep.* 28, 953–969. doi: 10.1039/c0np00032a
- Ge, G. B., Ning, J., Hu, L. H., Dai, Z. R., Hou, J., Cao, Y. F., et al. (2013). A highly selective probe for human cytochrome P450 3A4: isoform selectivity, kinetic characterization and its applications. *Chem. Commun.* 49, 9779–9781. doi: 10.1039/c3cc45250f
- Gowda, R. M., Cohen, R. A., and Khan, I. A. (2003). Toad venom poisoning: resemblance to digoxin toxicity and therapeutic implications. *Heart.* 89:e14. doi: 10.1136/heart.89.4.e14
- Han, L. Y., Wang, H. J., Si, N., Ren, W., Gao, B., Li, Y., et al. (2016). Metabolites profiling of 10 bufadienolides in human liver microsomes and their cytotoxicity variation in HepG2 cell. *Anal. Bioanal. Chem.* 408, 2485–2495. doi: 10.1007/s00216-016-9345-y
- Hsu, M. H., Savas, U., and Johnson, E. F. (2018). The X-Ray crystal structure of the human mono-oxygenase Cytochrome P450 3A5-ritonavir complex reveals active site differences between P450s 3A4 and 3A5. *Mol. Pharmacol.* 93, 14–24. doi: 10.1124/mol.117.109744
- Huang, H. M., Yang, Y. G., Lv, C., Chang, W. L., Peng, C. C., Wang, S. P., et al. (2015). Pharmacokinetics and tissue distribution of five bufadienolides from the shexiang baixin pill following oral administration to mice. *J. Ethnopharmacol.* 161, 175–185. doi: 10.1016/j.jep.2014.07.056
- Isin, E. M., and Guengerich, F. P. (2006). Multiple sequential steps involved in the binding of inhibitors to Cytochrome P450 3A4. *J. Biol. Chem.* 282, 6863–6874. doi: 10.1074/jbc.M610346200
- Kamano, Y., Kotake, A., Hashima, H., Inoue, M., Morita, H., Takeya, K., et al. (1998). Structure-cytotoxic activity relationship for the toad poison bufadienolides. *Bioorg. Med. Chem.* 6, 1103–1115. doi: 10.1016/S0968-0896(98)00067-4
- Krenn, L., and Kopp, B. (1998). Bufadienolides from animal and plant sources. *Phytochemistry* 48, 1–29. doi: 10.1016/S0031-9422(97)00426-3
- Li, Z. Y., Gao, H. M., Wang, J. H., Ting, Q. U., Chen, L. M., Wang, Z. M., et al. (2011). Inhibitory effect of total bufadienolides from toad venom against H22 tumor in mice and their metabolites. *China. J. Chin. Mater. Med.* 36, 2987–2992.
- Liu, S. B., Shi, X. F., Tian, X., Zhang, X. J., Sun, Z. Y., and Miao, L. Y. (2017). Effect of CYP3A4\*1G and CYP3A5\*3 polymorphisms on pharmacokinetics and pharmacodynamics of ticagrelor in healthy chinese subjects. *Front. Pharmacol.* 8:176. doi: 10.3389/fphar.2017.00176
- Liu, X. D., Hu, L. H., Ge, G. B., Yang, B., Ning, J., Sun, S. X., et al. (2014). Quantitative analysis of cytochrome P450 isoforms in human liver microsomes

- by the combination of proteomics and chemical probe-based assay. *Proteomics* 4, 1943–1951. doi: 10.1002/pmic.201400025
- Lu, Y. H., Hendrix, C. W., and Bumpus, N. N. (2012). Cytochrome P450 3A5 plays a prominent role in the oxidative metabolism of the anti-human immunodeficiency virus drug maraviroc. *Drug Metab. Dispos.* 40, 2221–2230. doi: 10.1124/dmd.112.048298
- Ma, X. C., Ning, J., Ge, G. B., Liang, S. C., Wang, X. L., Zhang, B. J., et al. (2011). Comparative metabolism of cinobufagin in liver microsomes from mouse, rat, dog, minipig, monkey, and human. *Drug Metab. Dispos.* 39, 675–682. doi: 10.1124/dmd.110.036830
- Ma, X. C., Zhang, B. J., Xin, X. L., Huang, S. S., Deng, S., Zhang, H. L., et al. (2009). Simultaneous quantification of seven major bufadienolides in three traditional Chinese medicinal preparations of chansu by HPLC-DAD. *Nat. Prod. Commun.* 4, 179–184.
- Mijatovic, T., and Kiss, R. (2013). Cardiotoxic steroids-mediated Na<sup>+</sup>/K<sup>+</sup>-ATPase targeting could circumvent various chemoresistance pathways. *Planta. Med.* 79, 189–198. doi: 10.1055/s-0032-1328243
- Ning, J., Hou, J., Wang, P., Wu, J. J., Dai, Z. R., Zou, L. W., et al. (2015a). Interspecies variation in phase I metabolism of bufalin in hepatic microsomes from mouse, rat, dog, minipig, monkey, and human. *Xenobiotica* 45, 954–960. doi: 10.3109/00498254.2015.1035359
- Ning, J., Yu, Z. L., Hu, L. H., Wang, C., Huo, X. K., Deng, S., et al. (2015b). Characterization of phase I metabolism of resibufogenin and evaluation of the metabolic effects on its antitumor activity and toxicity. *Drug Metab. Dispos.* 43, 299–308. doi: 10.1124/dmd.114.060996
- Raunio, H., Kuusisto, M., Juvonen, R. O., and Pentikäinen, O. T. (2015). Modeling of interactions between xenobiotics and cytochrome P450 (CYP) enzymes. *Front. Pharmacol.* 6:123. doi: 10.3389/fphar.2015.00123
- Salvador, J. A., Carvalho, J. F., Neves, M. A., Silvestre, S. M., Leitão, A. J., Silva, M. M., et al. (2013). Anticancer steroids: linking natural and semi-synthetic compounds. *Nat. Prod. Rep.* 30, 324–374. doi: 10.1039/c2np20082a
- Sevrioukova, I. F., and Poulos, T. L. (2012). Interaction of human cytochrome P4503A4 with ritonavir analogs. *Arch. Biochem. Biophys.* 520, 108–116. doi: 10.1016/j.abb.2012.02.018
- Sohl, C. D., Isin, E. M., Eoff, R. L., Marsch, G. A., Stec, D. F., and Guengerich, F. P. (2008). Cooperativity in oxidation reactions catalyzed by cytochrome P450 1A2: highly cooperative pyrene hydroxylation and multiphasic kinetics of ligand binding. *J. Biol. Chem.* 283, 7293–7308. doi: 10.1074/jbc.M709783200
- Westlind-Johnsson, A., Malmebo, S., Johansson, A., Otter, C., Andersson, T. B., Johansson, I., et al. (2003). Comparative analysis of CYP3A expression in human liver suggests only a minor role for CYP3A5 in drug metabolism. *Drug Metab. Dispos.* 31, 755–761. doi: 10.1124/dmd.31.6.755
- Wu, J. J., Cao, Y. F., Feng, L., He, Y. Q., Hong, J. Y., Dou, T. Y., et al. (2017). A naturally occurring isoform-specific probe for highly selective and sensitive detection of human Cytochrome P450 3A5. *J. Med. Chem.* 60, 3804–3813. doi: 10.1021/acs.jmedchem.7b00001
- Wu, J. J., Ge, G. B., He, Y. Q., Wang, P., Dai, Z. R., and Yang, L. (2016). Gomisin A is a novel isoform-specific probe for the selective sensing of human Cytochrome P450 3A4 in liver microsomes and living cells. *AAPS J.* 18, 134–145. doi: 10.1208/s12248-015-9827-4
- Xin, X. L., Zhan, L. B., Li, F. Y., Ma, X. C., Liu, K. X., Han, J., et al. (2009). Microbial transformation of bufotalin by *Alternaria alternata* AS 3.4578. *J. Asian Nat. Prod. Res.* 11, 7–11. doi: 10.1080/10286020802413197
- Ye, M., Guo, H., Guo, H., Han, J., and Guo, D. (2006). Simultaneous determination of cytotoxic bufadienolides in the Chinese medicine ChanSu by high-performance liquid chromatography coupled with photodiode array and mass spectrometry detections. *J. Chromatogr. B* 838, 86–95. doi: 10.1016/j.jchromb.2006.04.042
- Ye, M., Qu, G. Q., Guo, H. Z., and Guo, D. A. (2004). Novel cytotoxic bufadienolides derived from bufalin by microbial hydroxylation and their structure-activity relationships. *J. Steroid. Biochem. Mol. Biol.* 91, 87–98. doi: 10.1016/j.jsbmb.2004.01.010
- Yeh, J. Y., Huang, W. J., Kan, S. F., and Wang, P. S. (2003). Effects of bufalin and cinobufagin on the proliferation of androgen dependent and independent prostate cancer cells. *Prostate* 54, 112–124. doi: 10.1002/pros.10172
- Yusuke, O., Norie, M., Chihiro, Y., Makiko, S., Guengerich, F. P., and Hiroshi, Y. (2008). Drug interactions of thalidomide with midazolam and cyclosporine A: heterotropic cooperativity of human Cytochrome P450 3A5. *Drug Metab. Dispos.* 37, 18–23. doi: 10.1124/dmd.108.024679
- Zhang, D. M., Liu, J. S., Tang, M. K., Yiu, A., Cao, H. H., Jiang, L., et al. (2012). Bufotalin from venenum bufonis inhibits growth of multidrug resistant HepG2 cells through G(2)/M cell cycle arrest and apoptosis. *Eur. J. Pharmacol.* 692, 19–28. doi: 10.1016/j.ejphar.2012.06.045
- Zhang, J. W., Ge, G. B., Liu, Y., Wang, L. M., Liu, X. B., Zhang, Y. Y., et al. (2008a). Taxane's substituents at C3' affect its regioselective metabolism: different in vitro metabolism of cephalomannine and paclitaxel. *Drug Metab. Dispos.* 36, 418–426.
- Zhang, J. W., Liu, Y., Zhao, J. Y., Wang, L. M., Ge, G. B., Gao, Y., et al. (2008b). Metabolic profiling and Cytochrome P450 reaction phenotyping of medroxyprogesterone acetate. *Drug Metab. Dispos.* 36, 2292–2298. doi: 10.1124/dmd.108.022525
- Zhang, X., Ye, M., Dong, Y. H., Hu, H. B., Tao, S. J., Yin, J., et al. (2011). Biotransformation of bufadienolides by cell suspension cultures of *Saussurea involucrate*. *Phytochemistry* 72, 1779–1785. doi: 10.1016/j.phytochem.2011.05.004
- Zhu, Y. R., Xu, Y., Fang, J. F., Zhou, F., Deng, X. W., and Zhang, Y. Q. (2014). Bufotalin-induced apoptosis in osteoblastoma cells is associated with endoplasmic reticulum stress activation. *Biochem. Biophys. Res. Commun.* 451, 112–118. doi: 10.1016/j.bbrc.2014.07.077

**Conflict of Interest Statement:** The authors declare that the research was conducted in the absence of any commercial or financial relationships that could be construed as a potential conflict of interest.

Copyright © 2019 Dai, Ning, Sun, Wang, Zhang, Ma, Zou, Hou, Wu, Ge, Sun and Yang. This is an open-access article distributed under the terms of the Creative Commons Attribution License (CC BY). The use, distribution or reproduction in other forums is permitted, provided the original author(s) and the copyright owner(s) are credited and that the original publication in this journal is cited, in accordance with accepted academic practice. No use, distribution or reproduction is permitted which does not comply with these terms.